PHYSICAL REVIEW B, VOLUME 65, 064441

# Nonequivalence of chemical and hydrostatic pressures: $A_{1g}$ and $E_g$ frequencies and Stokes shift of $Mn^{2+}$-doped perovskites

M. T. Barriuso,[1] M. Moreno,[2] and J. A. Aramburu[2]
[1]*Departamento de Física Moderna, Universidad de Cantabria, Avda. Los Castros s/n, 39005 Santander, Spain*
[2]*Departamento de Ciencias de la Tierra y Física de la Materia Condensada, Universidad de Cantabria, Avda. Los Castros s/n, 39005 Santander, Spain*

(Received 26 March 2001; revised manuscript received 2 August 2001; published 24 January 2002)

The frequency of $A_{1g}$ and $E_g$ modes of $MnF_6{}^{4-}$ in cubic $ABF_3$ ($A$: K; B: Mg, Zn and $A$: Rb, Cs; $B$: Cd, Ca) perovskites has been derived through density functional calculations on $MnF_6A_8B_6{}^{16+}$ clusters which reproduce the experimental impurity-ligand distance $R_e$. Both frequencies are found to experience a drastic decrement on passing from $KMgF_3:Mn^{2+}$ ($\hbar\omega_A = 556\ cm^{-1}$, $\hbar\omega_E = 456\ cm^{-1}$) to $CsCdF_3:Mn^{2+}$ ($\hbar\omega_A = 317\ cm^{-1}$, $\hbar\omega_E = 239\ cm^{-1}$) despite the fact that $R_e$ increases *only* by 5%, leading to *effective* Grüneisen constants (called $\gamma_A^c$ and $\gamma_E^c$) around 3.0 along the series. This figure is 60% higher than the usual Grüneisen constant $\gamma_A$ calculated for a *given system* like $KMgF_3:Mn^{2+}$ or $KZnF_3:Mn^{2+}$ when hydrostatic pressure is applied. For supporting this relevant result the value of $\gamma_A$ for $CrF_6{}^{3-}$ in a fluoroelpasolite has been calculated as well. The obtained value $\gamma_A = 2.1$ is close to the experimental one ($\gamma_A = 1.9$) derived in $K_2NaGaF_6:Cr^{3+}$ by combined optical and Raman measurements. As a salient feature, the increase of the Stokes shift when $R_e$ increases observed along the $ABF_3:Mn^{2+}$ series is now well explained through the bigger variations of $A_{1g}$ and $E_g$ frequencies induced by the chemical pressure in comparison to those coming from an hydrostatic pressure on a given system. The difference between $\gamma_A^c$ and $\gamma_A$ is discussed through a simple model that emphasizes the role played by the coupling of the $MnF_6{}^{4-}$ complex to the lattice. The influence of chemical and hydrostatic pressures upon the luminescence efficiency is also briefly discussed. Attention is addressed to the method of calculating impurity-associated Grüneisen constants using clusters. Recent results on $Cr^{3+}$ in several cubic chloroelpasolites that support the present conclusions are briefly discussed as well.

DOI: 10.1103/PhysRevB.65.064441 PACS number(s): 75.30.−m, 71.55.−i, 78.55.−m, 63.20.Pw

## I. INTRODUCTION

The presence of a transition-metal (TM) impurity in an insulating material leads to the appearance of physicochemical properties which are absent in the pure host lattice and may be useful for applied devices such as solid-state lasers, storage phosphors, etc. Despite a doped material being certainly more complex than a pure one, it was first pointed out by Sugano and Shulman[1] that the *electronic properties* due to an impurity in an *insulating* lattice can be understood to a good extent *only* on the basis of the $ML_N$ complex formed by the impurity $M$ and the $N$ nearest anions.[2] This relevant conclusion means that, in thermodynamic equilibrium, a pure electronic parameter $P_{\mathrm{el}}$ related to the impurity (like the energy of an optical transition or the $g$ factor) depends, in a good first approximation, only on the equilibrium impurity-ligand distance $R_e$ as well as on the temperature $T$. This idea is correct provided (i) the active electrons of the complex are localized inside the $ML_N$ complex and (ii) the electrostatic potential $V_R$, due to the rest of the lattice upon the active electrons, is essentially flat inside the complex region. Both conditions are fulfilled for divalent and trivalent TM impurities placed substitutionally in cubic insulating lattices.[3] When the TM impurity is located in sites of lower symmetry, it is, however, necessary to include the effects of $V_R$ for a proper understanding of the center.[4]

If apart from temperature a parameter $P_{\mathrm{el}}$ only depends on $R_e$, $\Delta P_{\mathrm{el}}$ variations can thus be obtained using either a hydrostatic pressure or a change of the host lattice (chemical pressure) producing the *same* variation $\Delta R_e$ in the impurity-ligand distance. The equivalence between a hydrostatic and a chemical pressure has been demonstrated experimentally as far as electronic properties are concerned. For instance, the dependence of $10Dq$ upon $R_e$ has been measured experimentally either by means of a hydrostatic pressure on a given doped lattice or through different host lattices containing the *same* $ML_N$ complex.[5–11]

Writing

$$10Dq = KR_e^{-n}, \tag{1}$$

it turns out that *similar* values of the exponent $n$ are derived through *both* procedures.

As regards the local vibrations associated with a given impurity, they cannot, however, be understood *only* in terms of the $ML_N$ complex. For instance, in a $\sigma$ mode of vibration the ligands do *also* interact with the first host lattice cations (placed along the metal-ligand directions) whose nature is only modified when the host lattice changes. Therefore the effects of the chemical pressure on a $ML_N$ complex are not necessarily equivalent to those arising from the hydrostatic pressure on a given doped compound when the vibrations associated with an impurity are concerned. This idea can also be of importance in the case of parameters (such as the Stokes shift or the Huang-Rhys factors) depending on the coupling between an excited electronic state and the local vibrations.[12–17] Along this line the effects of both kind of pressures upon the luminescence quenching also deserve an investigation.

Searching to explore these attractive questions, the variation of the $A_{1g}$ and $E_g$ frequencies associated with the

$MnF_6{}^{4-}$ complex in cubic $ABF_3$ ($B$=divalent element) fluoroperovskites is derived in the present work through density functional theory (DFT) calculations on clusters centered at $Mn^{2+}$. Results for $KBF_3:Mn^{2+}$ ($B$: Mg, Zn) and $ABF_3:Mn^{2+}$ ($A$: Rb, Cs; $B$: Cd, Ca) are reported. For comparison purposes the effects of a hydrostatic pressure on the systems $KMgF_3:Mn^{2+}$ and $KZnF_3:Mn^{2+}$ are also explored.

The ensemble of *cubic* fluoroperovskites doped with $Mn^{2+}$ can be considered as *model systems*[18–20] where the impurity-ligand distance has been determined through *three independent* methods.[2,22,6] Moreover, recent DFT calculations on 21-atom clusters[23] lead to values of the equilibrium impurity-ligand distance $R_e$ which are coincident, within experimental uncertainties, with those derived from electron paramagnetic resonance (EPR),[22] optical,[6] and extended x-ray absorption fine structure (EXAFS)[21] data at ambient pressure.

Experimental information on vibration modes coupled to the first excited state of $MnF_6{}^{4-}$ in fluoroperovskites comes from the low-temperature optical spectra.[24] For instance, in $KMgF_3:Mn^{2+}$ a mode of 570 $cm^{-1}$ frequency has been revealed in the high-resolution emission spectrum. Although that frequency is close to that of the $LO_3$ mode of the pure lattice, that mode has been associated[25] with a local or resonant mode because its value is shifted to 540 $cm^{-1}$ in the absorption spectrum.

The substitution of a host lattice by another one (chemical pressure on the complex) leads to variations of both $\omega_i$ ($i=A,E$) and $R_e$ parameters (termed as $\Delta_c\omega_i$ and $\Delta_c R_e$, respectively), and thus it allows one to define an *effective* Grüneisen parameter $\gamma_i^c$ through the expression

$$3\gamma_i^c=\frac{\Delta_c\omega_i}{\Delta_c R_e}\frac{R_e}{\omega_i}. \tag{2}$$

Comparison of this *effective* constant $\gamma_i^c$ with the actual Grüneisen parameter $\gamma_i$ corresponding to *a given* doped compound can thus be used for describing in a simple way the differences between chemical and hydrostatic pressures.

Particular attention is paid through this work to the variation of the Stokes shift ($E_S$) associated with the ${}^4T_1\rightarrow{}^6A_1$ luminescent transition of $MnF_6{}^{4-}$ along the fluoroperovskite series that has been studied experimentally.[19] Such experimental results show that $E_S$ increases as far as the actual value of $R_e$ increases along the series. Moreover, an analysis of such results indicates that the average value of $\gamma_i^c$ ($i=A,E$) along the series can be around 3 indeed. This figure is higher than the *usual* values of $\gamma_i$ measured for a given compound. In this sense the *average* $\overline{\gamma}$ value derived from thermal expansion data[26,27] for pure $KZnF_3$ and $CsCaF_3$ is equal to 1.1. Moreover, the Grüneisen parameters associated with the local $A_{1g}$ and $E_g$ modes of $K_2NaGaF_6:Cr^{3+}$ have been derived through combined optical and Raman measurements under pressure.[28] The obtained results ($\gamma_A=1.85$ and $\gamma_E=2.1$) point out that even in the case of the stretching modes the Grüneisen parameters are clearly smaller than 3. Therefore, for supporting the study carried out on $MnF_6{}^{4-}$ in fluoroperovskites, the Grüneisen constant $\gamma_A$ for $CrF_6{}^{3-}$ in the elpasolite lattice $K_3CrF_6$ has been calculated in the present work as well.

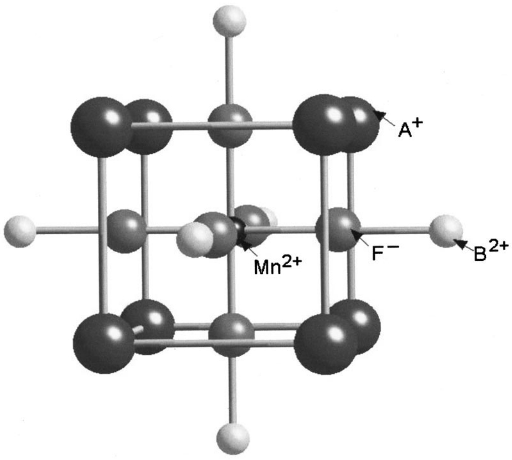

FIG. 1. Cluster of 21 atoms used in the ADF calculation of $ABF_3:Mn^{2+}$ systems.

## II. THEORETICAL

The properties due to $Mn^{2+}$-doped fluoroperovskites have been calculated by means of finite clusters. As the boundary condition, the surface atoms of the cluster are fixed at their experimental host lattice positions. This procedure provides a reasonable insight into the properties associated with an *impurity* provided (i) the active electrons are localized in a small region compared to the cluster size and (ii) impurity-induced local relaxations are important only in a domain whose size is again smaller than that of the cluster. For the present work $MnF_6A_8B_6{}^{16+}$ clusters (Fig. 1) have been used. As previously discussed,[23] this cluster reasonably fulfills the two conditions for the six fluoroperovskites. In particular, less than 5% of the charge associated with unpaired electrons is found to reside outside the $MnF_6{}^{4-}$ complex

Calculations of the ground-state energy for different values of the metal-ligand distance $R$ have been carried out using the Amsterdam density functional (ADF) code[29] and the generalized gradient approximation (GGA) by means of the Becke-Perdew functional.[30,31] The effects of the electrostatic potential due to the rest of the ions not included in the $MnF_6A_8M_6{}^{16+}$ cluster have been considered in all the calculations. The basis set of the best quality in the ADF code has been employed. More details can be found elsewhere.[23]

It has recently been shown that using $MnF_6A_8B_6{}^{16+}$ clusters the obtained $R_e$ values for the series of $Mn^{2+}$-doped fluoroperovskites coincide, within the experimental uncertainties, with those derived from the analysis of the experimental isotropic superhyperfine constant $A_s$, the $10Dq$ parameter, and available EXAFS results.[23] For calculating the local $A_{1g}$ and $E_g$ frequencies through the $MnF_6A_8B_6{}^{16+}$ cluster, it has been assumed, in a first approximation, that only the ligand displacements are involved in the corresponding normal coordinates. This assumption is quite reasonable in the case of elpasolite lattices (where $A_{1g}$ and $E_g$

modes of the complex are also[13] lattice modes at $\mathbf{k}=0$), but can only be taken as a first step in the case of perovskites. A description of $A_{1g}$ and $E_g$ modes is given in Ref. 32.

In the self-consistent solution of Kohn-Sham equations[33] the initial potential used in the $n$ step, $V_n^i$, leads to a final potential $V_n^f$ once such equations are solved. The initial potential $V_{n+1}^i$ employed in the $n+1$ step is taken as

$$V_{n+1}^i=(1-\varepsilon)V_n^i+\varepsilon V_n^f, \tag{3}$$

where the mixing coefficient $\varepsilon$ is usually taken equal to 0.2. In the calculations on $\mathrm{K}B\mathrm{F}_3:\mathrm{Mn}^{2+}$ ($B$: Mg, Zn) and $A\mathrm{CdF}_3:\mathrm{Mn}^{2+}$ ($A$: Rb, Cs) the convergence was perfect and reached for an error parameter of the ADF code equal to $10^{-6}$. Problems were found however, to achieve a proper convergence in the case of $A\mathrm{CaF}_3:\mathrm{Mn}^{2+}$ ($A$: Rb, Cs) systems. In these two systems convergence was obtained using an error parameter bigger than $30\times10^{-6}$ and $\varepsilon$ lying between 0.06 and 0.35. Moreover, for $R<R_e$ convergence was reached only when $R_e-R<8$ pm. This situation could be related to the presence of an $a_1$ "ghost orbital" lying in the antibonding $3d$ orbital region of $\mathrm{Mn}^{2+}$ as pointed out by other workers.[34,35] In view of these facts the present analysis is based mainly on results obtained for the $\mathrm{K}B\mathrm{F}_3:\mathrm{Mn}^{2+}$ ($B$: Mg, Zn) and $A\mathrm{CdF}_3:\mathrm{Mn}^{2+}$ ($A$: Rb; Cs) systems. The main trend emerging from these results is, however, followed by those coming from calcium perovskites as indicated later.

For the whole analyzed systems, we have verified that the fitting of the $E(R)$ curve by polynomials of different degree leads essentially to the *same* values of second and third derivatives at $R=R_e$. Here $R$ is the fluoride coordinate along the $\langle 100\rangle$ directions.

The volume dependence of a vibrational frequency $\omega_i$ of a given system is quantified through the associated Grüneisen parameter $\gamma_i$. For an octahedral molecule the volume is just determined by the metal-ligand distance $R_e$, and then $\gamma_i$ is defined by the relation

$$\gamma_i=\frac{\partial L\omega_i}{\partial LV}=\frac{1}{3}\,\frac{\partial L\omega_i}{\partial LR_e}. \tag{4}$$

Thus the Grüneisen parameter $\gamma_i$ plays a key role for understanding the effects of an hydrostatic pressure upon $\omega_i$. Attention has to be paid, however, to the calculation of $\gamma_i$ ($i=A,E$) for $\mathrm{MnF_6}^{4-}$ embedded in a lattice. To get an insight into $\gamma_i$ ($i=A,E$) by means of calculations on a cluster, one has to determine the changes experienced by $R_e$ and the $\omega_i$ ($i=A,E$) when the cluster size is modified, but its geometry is frozen. In the cluster depicted in Fig. 1 the size is controlled by the distance $R_S$ between the impurity and six $B^{2+}$ ions lying in $\langle 100\rangle$ directions. In the perfect host lattice at zero pressure, $R_S$ is equal to the perovskite lattice parameter $a$. When the cluster size is changed, for a given $R_S$ value the position of the 14 "surface" ions of the cluster is taken to be that corresponding to a perovskite lattice with $a=R_S$. Through this approximation, the ground state energy $E$ of the cluster depends only on the $R$ and $R_S$ *variables*. From the $E(R,R_S)$ function the equilibrium metal-ligand distance $R_e$ or the $\omega_A$ frequency can be derived for *each value* of the cluster size. At *a given* $R_S$ value, termed $R_S^e$, the equilibrium $R_e$ distance is just determined by the condition

$$\left(\frac{\partial E(R,R_S=R_S^e)}{\partial R}\right)_{R=R_e}=0 \tag{5}$$

and then the force constant $k_A$ and frequency $\omega_A$, *corresponding* to a given equilibrium distance $R_e$, are just given by

$$k_A=6M_L\omega_A^2=\left[\frac{\partial^2E(R;R_S=R_S^e)}{\partial R^2}\right]_{R=R_e} \tag{6}$$

where $M_L$ means the mass of one of six ligand ions. Once the value of $\omega_A$ for different $R_e$ distances is known, $\gamma_A$ is easily derived. At zero pressure, $R_S^e$ is taken equal to the experimental value in the perfect host lattice. For the present systems this assumption is reasonable as the relaxation of the ligand shell is smaller than 4.5% and, as discussed in Ref. 23, an estimation based on the theory of elasticity leads to a relative variation of the third neighbors distance smaller than 0.7%.

A similar procedure to that followed for $\mathrm{MnF_6}^{4-}$ in fluoroperovskites has been used for calculating $\gamma_A$ in the case of $\mathrm{CrF_6}^{3-}$ in the $\mathrm{K_3CrF_6}$ elpasolite lattice where two close complexes do not share any common ligand. According to a previous work,[36] calculations are carried out on a $\mathrm{CrF_6K_8K_6}^{11+}$ cluster centered at the chromium ion.

It is worth noting that a different (and, in general, incorrect) value of $\gamma_A$ is obtained when the surface atoms are kept fixed at a distance $R_f$ (which can correspond to the perfect host lattice) from the central cation and only the ligands are allowed to follow an external pressure.[37,36] The constant calculated by this *artificial* procedure will be hereafter denoted by $\gamma_A(f)$. The difference between $\gamma_A(f)$ and $\gamma_A$ is discussed in Sec. III D.

## III. RESULTS AND DISCUSSION

### A. Vibrational frequencies for $\mathrm{MnF_6}^{4-}$ in perovskites

The $R$ dependence of the ground-state energy, $E(R)$, obtained for the $\mathrm{MnF_6K_8Mg_6}^{16+}$ cluster in $\mathrm{KMgF_3}$ and the $\mathrm{MnF_6Cs_8Cd_6}^{16+}$ cluster in $\mathrm{CsCdF_3}$ are both portrayed in Fig. 2. It can be noticed that the curvature around the minimum at $R_e=2.057$ Å for the former system is much higher than that corresponding to the latter one whose minimum appears at $R_e=2.156$ Å.

The values of calculated $\omega_A$ and $\omega_E$ frequencies for $\mathrm{K}B\mathrm{F}_3:\mathrm{Mn}^{2+}$ ($B$: Mg, Zn) and $A\mathrm{CdF}_3:\mathrm{Mn}^{2+}$ ($A$: Rb, Cs) together with the corresponding equilibrium distances are displayed in Table I. For comparison purposes the $R_e$ values derived[22] from the experimental isotropic superhyperfine constant $A_s$ are also shown. As previously pointed out,[23] the calculated $R_e$ values by means of 21-atom clusters agree with those derived from the analysis of experimental data within experimental uncertainties.

The reported values in Table I indicate that the replacement of a fluoroperovskite lattice by another one leads to

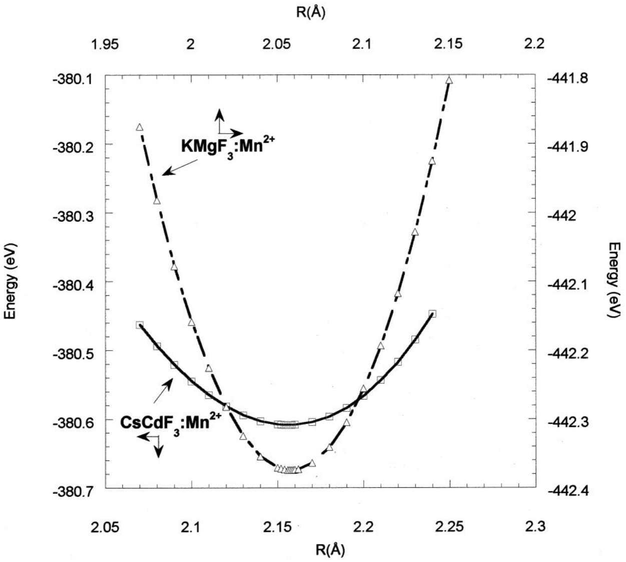

FIG. 2. Calculated ground-state energy for $KMgF_3:Mn^{2+}$ and $CsCdF_3:Mn^{2+}$ for different values of the $Mn^{2+}$-$F^-$ distance $R$. Note that the origin of the $R$ coordinate corresponding to $CsCdF_3:Mn^{2+}$ is shifted by 0.10 Å with respect to that for $KMgF_3:Mn^{2+}$.

remarkable changes of $\omega_A$ and $\omega_E$ frequencies. For instance, $R_e$ for $CsCdF_3:Mn^{2+}$ is found to be only 5% higher than that for $KMgF_3:Mn^{2+}$, while the associated $\omega_A$ frequency is calculated to be 43% smaller. A similar variation is found for the Jahn-Teller frequency $\omega_E$. Systems for which $R_e > 2.12$ Å are found to possess $\omega_A$ and $\omega_E$ values much smaller than those corresponding to $KBF_3:Mn^{2+}$ $(B\text{:Mg, Zn})$. This trend is not altered by the results on $RbCaF_3:Mn^{2+}$ $(R_e = 2.125$ Å$)$ and $CsCaF_3:Mn^{2+}$ $(R_e = 2.155$ Å$)$ obtained, however, under worse technical conditions. In both cases $\hbar\omega_A$ would lie in the 310–350 $cm^{-1}$ domain.

Comparing the results displayed in Table I for $CsCdF_3:Mn^{2+}$ and $KMgF_3:Mn^{2+}$ $\gamma_A^c = 3.2$ and $\gamma_E^c = 2.85$ values are derived. This result already points out that the effective Grüneisen parameters $\gamma_A^c$ and $\gamma_E^c$ can attain values very close to 3 indeed.

The calculated variation of $\omega_A$ along the series of $ABF_3:Mn^{2+}$ systems is certainly bigger than that experienced by the $LO_3$ frequency of the corresponding host lattice.[27] For instance, the $LO_3$ frequency for $KMgF_3$ and $CsCaF_3$ is equal to 551 and 449 $cm^{-1}$, respectively, which means a variation of *only* 18%.

For the studied systems in Table I the frequency $\omega_A$ of the symmetric mode is found to be bigger than that of the Jahn-Teller mode, which also exhibits a stretching character. Qualitatively, this trend can simply be understood looking at the vibrations in a $ML_6$molecule assuming two-body central forces.[38,39] Let us consider the $Q_\epsilon$ $(\sim x^2 - y^2)$ coordinate of the $E_g$ mode. The two adjacent ligands placed initially at $(R_e,0,0)$ and $(0,R_e,0)$ are moved to $(R_e + \delta,0,0)$ and $(0,R_e - \delta,0)$, respectively. Thus the distance between both ions is kept *in first order* if $|\delta| \ll R_e$ at variance with what happens for the $A_{1g}$ mode. Therefore, there is no contribution to $\omega_E$ from this ligand-ligand force constant.

Vibrations associated with the impurity are revealed[24] in high-resolution luminescence spectra of $KMgF_3:Mn^{2+}$ and $KZnF_3:Mn^{2+}$. In both cases a clear replica of a mode whose frequency is 570 $cm^{-1}$ for $KMgF_3:Mn^{2+}$ can be observed. In view of the results of Table I, that mode could be ascribed in a first approximation to the symmetric vibration of $F^-$ ligands. On passing from $KMgF_3:Mn^{2+}$ to $KZnF_3:Mn^{2+}$ the experimental frequency of such a mode experiences a 30-$cm^{-1}$ redshift which is smaller than that calculated in Table I. It is worth noting that the increase in $R_e$ (termed $\Delta R_e$) on going from $KMgF_3:Mn^{2+}$ to $KZnF_3:Mn^{2+}$ is calculated to be equal to 3 pm. This figure is consistent with $R_e$ values derived the experimental $A_s$ provided the *experimental uncertainties* are taken into account. If $\Delta R_e$ is actually closer to 1 pm, one would expect a redshift for $\hbar\omega_A$ around 30 $cm^{-1}$ when $KMgF_3$ is replaced by $KZnF_3$.

No direct measurements have been carried out in the case of the Jahn-Teller frequency $\omega_E$. The calculated $\hbar\omega_E$ values in Table I exhibit, however, a trend which is certainly comparable to the estimations reported[12,24] for $KMgF_3:Mn^{2+}$ $(R_e = 207$ pm, $\hbar\omega_E = 390$ $cm^{-1})$ and $RbMnF_3$ $(R_e = 212$ pm, $\hbar\omega_E = 280$ $cm^{-1})$.

### B. Grüneisen constant $\gamma_A$ for $KBF_3:Mn^{2+}$ $(B\text{:Mg, Zn})$ and $K_3CrF_6$

Changes of the $A_{1g}$ frequency of *a given* $KBF_3:Mn^{2+}$ system $(B\text{:Mg, Zn})$ produced by a modification of the equilibrium distance have also been studied. The main results collected in Fig. 3 indicate that $d\omega_A/dR_e$ is negative and thus $\gamma_A$ is positive. This situation is usually found for stretching modes of molecules and crystals.[40–42] Acoustic bending modes in silicon lead, however, to negative values

TABLE I. $A_{1g}$ and $E_g$ vibration frequencies for $Mn^{2+}$-doped fluoroperovskites. The equilibrium distances obtained from ADF calculations and from the experimental $A_s$ value are also included.

| | | Equilibrium distance $R_e$ (Å) | | Frequencies $(cm^{-1})$ | |
|---|---|---|---|---|---|
| Lattice | Lattice parameter (Å) | From ADF calc. | From expt. $A_s$ | $A_{1g}$ mode $\omega_A$ | $E_g$ mode $\omega_E$ |
| $KMgF_3$ | 3.973 | 2.057 | 2.07 | 556 | 456 |
| $KZnF_3$ | 4.054 | 2.086 | 2.08 | 454 | 387 |
| $RbCdF_3$ | 4.400 | 2.127 | 2.12 | 353 | 285 |
| $CsCdF_3$ | 4.464 | 2.156 | 2.14 | 317 | 239 |

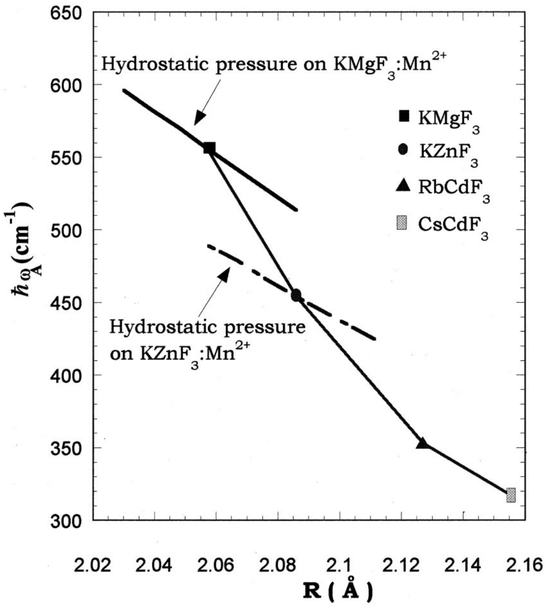

FIG. 3. Variation of $\hbar\omega_A$ along the series of cubic fluoroperovskites doped with Mn$^{2+}$. Calculated hydrostatic pressure effect on $\hbar\omega_A$ for K$B$F$_3$:Mn$^{2+}$ ($B$=Mg,Zn) systems is also showed for comparison.

of the Grüneisen constant,[41,42] which is in turn responsible for the negative thermal expansion coefficient below 150 K.

As a salient feature, it can be noticed that for the same $\Delta R_e$ value the variation $\Delta\hbar\omega_A$ obtained for a given compound doped with Mn$^{2+}$ under hydrostatic pressure is certainly smaller than through the replacement of the host lattice. More precisely, the Grüneisen constant $\gamma_A$ is found to be practically equal to 1.8 for both KMgF$_3$:Mn$^{2+}$ and KZnF$_3$:Mn$^{2+}$ systems. It is worth noting that using the same procedure as for KMgF$_3$:Mn$^{2+}$ and KZnF$_3$:Mn$^{2+}$ the Grüneisen constant $\gamma_A$ for CrF$_6{}^{3-}$ in the K$_3$CrF$_6$ elpasolite has also been calculated. The obtained value $\gamma_A = 2.1$ is close to the experimental one ($\gamma_A = 1.9$) derived by Dolan *et al.*[28] in K$_2$NaGaF$_6$:Cr$^{3+}$. It is worthwhile to remark that if $\gamma_A$ is derived from the calculated potential curve for the cluster with the six surface ions *fixed* at the lattice positions at zero pressure, then it is found that $\gamma_A(f) = 1.1$. Why the $\gamma_A$ value obtained through a reasonable calculation is higher than $\gamma_A(f)$ is analyzed in Sec. III. D.

In the present calculations on KMgF$_3$:Mn$^{2+}$ or KZnF$_3$:Mn$^{2+}$, it is found that when the cluster size is changed by a quantity $\Delta R_s$, then the relative variation undergone by the metal-ligand distance is given by $\Delta R_e/R_e = b(\Delta R_s/R_s)$, where $b = 0.87$. This figure means that ligands follow the motion of outer ions rather closely. In the case of the K$_3$CrF$_6$ elpasolite, $b$ is found to be 0.4, suggesting that the local compressibility of CrF$_6{}^{3-}$ is bigger than that of the whole lattice. A similar situation has been found[43] in MgO:Cr$^{3+}$.

### C. Stokes shift for Mn$^{2+}$-doped fluoroperovskites

The luminescence due to MnF$_6{}^{4-}$ complexes in fluorides comes only[44,12,6] from the first excited state $^4T_{1g}$. The corresponding Stokes shift $E_s$ strongly depends upon the $\omega_i$ ($i = A,E$) frequencies.[14,15] Therefore, one can expect that the big difference between $\gamma_A$ and $\gamma_A^c$ obtained through the present calculations plays an important role for explaining the *variation* of $E_s$ measured through the series of cubic fluoroperovskites doped with Mn$^{2+}$. As shown in Fig. 4, the experimental Stokes shift[19] increases as far as $R_e$ increases in the fluoroperovskites series.

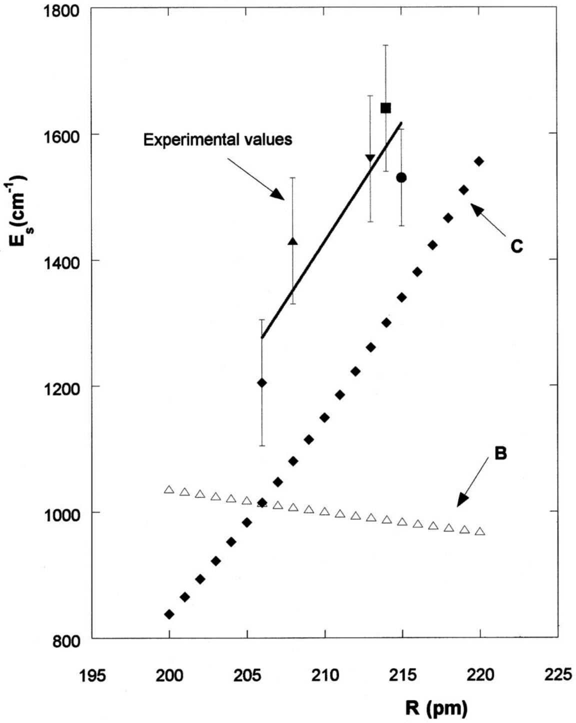

FIG. 4. Calculated Stokes shift values for two different $\gamma$ values, 1.8 ($B$ line) and 3 ($C$ line), respectively. Experimental $E_S$ values for different host lattices are also shown for comparison. ◆: KMgF$_3$. ▲: KZnF$_3$. ▼: RbCdF$_3$. ■: RbCaF$_3$. ●: CsCaF$_3$.

Theoretically, the Stokes shift for $d^5$ or $d^3$ ions placed in lattices like elpasolites or perovskites can simply by written[13,15] as

$$E_S = E_S(A) + E_S(E) \tag{7}$$

where $E_s(A)$ and $E_s(E)$ denote the contribution arising from the coupling of the first electronic excited state with the symmetric and the Jahn-Teller mode, respectively. The expression of $E_s(i)$ ($i = A,E$) in terms of the corresponding coupling constant, $V_i$, and the $\omega_i$ ($i = A,E$) frequency is formally the same for both modes:[45,12,15]

$$E_S(i) = \frac{V_i^2}{M_L\omega_i^2} = 2S_i\hbar\omega_i, \tag{8}$$

where $S_i$ is the associated Huang-Rhys factor. As to $V_i$ for the $^4T_{1g}$ state of MnF$_6{}^{4-}$, it has been shown[15,14] that its dependence on $R_e$ around 212 pm can be described by

$$V_i = C_i R_e{}^{-n_i}. \tag{9}$$

The exponents $n_A$ and $n_E$ are found to be very similar[15] for $\mathrm{MnF_6}^{4-}$ as well as for $\mathrm{CrF_6}^{3-}$. Moreover, $n_A=n+1$, where the exponent $n$ reflects the dependence of $10Dq$ upon $R_e$ through Eq. (1). Microscopically, the strong dependence of $10Dq$ upon $R_e$ in complexes like $\mathrm{MnF_6}^{4-}$ has been shown to be related to the $3d$-$2s(F)$ hybridization in the antibonding $e_g$ $(\sim x^2-y^2, 3z^2-r^2)$ orbital.[46,47]

On these bases, the $R_e$ dependence of $E_s$ found experimentally[19] has to be related to the variations of frequencies along the series and also to the $R_e$ dependence of the coupling constants $V_A$ and $V_E$. Calculated values of $E_s$ as a function of $R_e$ by means of Eqs. (6)–(8) are also included in Fig. 4. According to the analysis performed in Ref. 15, the employed values of $V_A$ and $V_E$ for $\mathrm{KMgF_3{:}Mn^{2+}}$ ($R_e=206$ pm) are $V_A=95\ \mathrm{cm^{-1}/pm}$ and $V_E=75\ \mathrm{cm^{-1}/pm}$. As to the exponents $n_A$ and $n_E$ involved in the $R_e$ dependence of $E_s$, the values $n_A=6$ and $n_E=5.5$ are used.[15] The frequencies for $\mathrm{KMgF_3{:}Mn^{2+}}$ are taken equal to $\hbar\omega_A=550\ \mathrm{cm^{-1}}$ and $\hbar\omega_E=450\ \mathrm{cm^{-1}}$. For simulating their variation along the fluoroperovskite series, it has first been assumed that $\gamma_A^c$ and $\gamma_E^c$ are equal to the Grüneisen constant $\gamma_A=1.8$ calculated for $\mathrm{K}B\mathrm{F_3{:}Mn^{2+}}$ ($B$:Mg, Zn) systems. It can be seen in Fig. 4 that the calculated values of $E_s$ derived from the latter assumption fail to reproduce the trend experimentally observed.[19] In fact, the derived $E_s$ values, obtained assuming $\gamma_A^c\cong\gamma_E^c=1.8$, do not give rise to a significant increase of the Stokes shift when $R_e$ increases, but rather to a slow decrement. As shown also in Fig. 4, this big discrepancy is, however, overcome by putting $\gamma_A^c\cong\gamma_E^c=3$, as derived from the present calculations in Sec. III A. This relevant result can easily be rationalized through Eqs. (7) and (8), implying that a contribution like $E_s(A)$ should be proportional to $R_e^{p_A}$ where the exponent $p_A$ is given by

$$p_A=6\gamma_A^c-2n_A \tag{10}$$

if the host lattice chemical pressure is modified, while

$$p_A=6\gamma_A-2n_A \tag{11}$$

when a hydrostatic pressure is applied on a given compound. Therefore, if $n_A\cong 6$ and $\gamma_A=1.8$, then $p_A=-1.2$, which means that an applied hydrostatic pressure on a system like $\mathrm{KMgF_3{:}Mn^{2+}}$ would lead to a *slow increase* of $E_s(A)$. By contrast, when the chemical pressure along the fluoroperovskite series is varied it turns out that the calculated value $\gamma_A^c=3$ leads to $p_A\cong 6$ and thus to an important increase of $E_s$ when $R$ increases. This agreement can thus be viewed as an experimental proof, though indirect, of the conclusions in Secs. III A and III B. Therefore, for $\mathrm{MnF_6}^{4-}$ in fluoroperovskite lattices, the changes in $A_{1g}$ and $E_g$ frequencies due to the chemical pressure appear to be bigger indeed than those coming from an hydrostatic pressure on a given compound.

The results gathered in Fig. 4 also predict that the Stokes shift of a system like $\mathrm{KMgF_3{:}Mn^{2+}}$ would be little affected by an applied hydrostatic pressure. Further experimental work is desirable to explore this prediction.

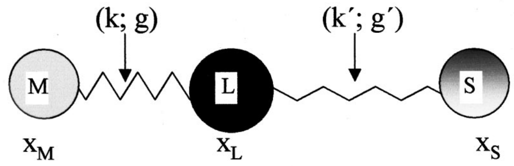

FIG. 5. Simple model representing three atoms ($M$, impurity metal atom: $L$, ligand atom; and $S$, "surface atom") connected by two springs with parameters (see text) $k,g$ and $k',g'$, respectively. $x_i$ ($i=M,L,S$) represents the position of atom $i$.

### D. Difference between $\gamma_A^c$, $\gamma_A$, and $\gamma_A(f)$: Insight through a simple model

The main differences between the three quantities $\gamma_A^c$, $\gamma_A$, and $\gamma_A(f)$ discussed in this work can be rationalized by means of a simple unidimensional model described in Fig. 5. In it, the atom at the origin representing the impurity is joined by an anharmonic spring to the ligand $L$, which in turn is joined to the surface atom by a different spring. The potential energy of the system including an external force acting on the surface atom is simply written as

$$E=\frac{1}{2}k(x_L-x_M-R_0)^2+\frac{1}{2}k'(x_S-x_L-R_0')^2+Fx_S-\frac{1}{6}g(x_L-x_M-R_0)^3-\frac{1}{6}g'(x_S-x_L-R_0')^3. \tag{12}$$

Here $x_L$ and $x_S$ mean the position of the ligand and surface atom, respectively, while the position of the impurity atom is fixed at $x_M=0$. The constants $k$ and $g$ ($k'$ and $g'$) are involved in the harmonic and anharmonic terms of the first (second) spring, while $R_0$ and $R_0'$ are the equilibrium positions associated with the two isolated springs. For each value of the force $F$, the equilibrium $x_L^e$ and $x_S^e$ values are determined in a first approximation by the conditions

$$k'(x_S^e-x_L^e-R_0')+F\approx 0, \tag{13}$$

$$k(x_L^e-R_0)-k'(x_S^e-x_L^e-R_0')\approx 0. \tag{14}$$

The force constant $k_A$ associated with such an equilibrium position is given by

$$k_A=\left(\frac{\partial^2 E}{\partial x_L^2}\right)_{\substack{x_L=x_L^e\\ x_S=x_S^e}}=k+k'-\left(g+g'\frac{k}{k'}\right)(x_L^e-R_0). \tag{15}$$

Therefore the change $\Delta k_A$ experienced by the force constant $k_A$ when $x_L^e$ is varied is just given by

$$\Delta k_A=-\left(g+g'\frac{k}{k'}\right)\Delta x_L^e. \tag{16}$$

In the calculation of $\gamma_A(f)$ the only variable is $x_L$ and the force $F$ has to be applied on the atom $L$ in order to modify $x_L^e$ while the atom $S$ is kept fixed at the perfect host lattice position termed $x_S^h$. In such a case Eq. (13) is not valid and the involved variation of $k_A$ termed $\Delta k_A(f)$ is simply given by

$$\Delta k_A(f) = -(g-g')\Delta x_L^e. \tag{17}$$

This fact stresses that if $\Delta x_L^e > 0$, then the anharmonic energy of the first spring decreases while that of the second one increases. Comparison between Eqs. (16) and (17) clearly shows that for the same $\Delta x_L^e$ variation $\Delta k_A(f) < \Delta k_A$ provided $g'$ is not negligible.

Let us now focus on the variation undergone by $k_A$ (called $\Delta_c k_A$) when the host lattice is modified. As a first approximation, we can assume that relaxation effects are important only for the ligand shell, while the surface atom remains at its host lattice position $x_S^h$. In this case the value of

$$k_A = \left(\frac{\partial^2 E}{\partial x_L^2}\right)_{\substack{x_L = x_L^e \\ x_S = x_S^h}}$$

for each lattice is also given by Eq. (14). Therefore, if the host lattice is changed, then

$$\Delta_c k_A = \Delta_c k' - g\Delta_c\left\{\left(1+\frac{g'}{g}\frac{k}{k'}\right)(x_L^e - R_0)\right\}, \tag{18}$$

which means that *even in the harmonic approximation* the replacement of a host lattice by another one can lead to variations of the force constant $k_A$ as $k'$ is modified. If the complex (simbolized by atoms $M$ and $L$) is, however, only weakly coupled to the rest of the lattice and thus $k' \ll k$, it is possible that, for the same $\Delta x_L^e$, $\Delta_c k_A$ is comparable to $\Delta k_A$ defined in Eq. (16). This would occur when $\Delta_c k' < g\Delta x_L^e$ assuming that $g'k/(gk')$ can be taken as a constant. A simple analysis of experimental $Mn^{2+}$-$F^-$ distances in fluoroperovskites through Eq. (14) leads, however, to $k'/k \approx 0.5$, pointing out the existence of a significant coupling between the complex and the lattice for the present cases. In the case of alkali halides or perovskites, $k'$ decreases[26,27] when the lattice parameter $a$ increases. As $x_L^e$ also increases following $a$, it turns out that the two contributions in Eq. (18) have the same sign and thus $\Delta_c k_A > \Delta k_A$.

### E. Quenching of the luminescence in $Mn^{2+}$-doped fluorides

The influence of chemical or hydrostatic pressures upon the luminescence efficiency deserves some discussion. Since the first work by Dexter *et al.*,[48] it is known that the luminescence quenching is partially governed by the $\Lambda$ parameter defined by

$$\Lambda = \frac{E_s}{2E_G}, \tag{19}$$

where $E_G$ means the energy difference between the emitting first excited state and the ground one. In the case of $Mn^{2+}$ in an octahedral field $E_G$ is given in a first approximation by

$$E_G = 10B + 6C - 10Dq, \tag{20}$$

where $B$ and $C$ are the usual Racah parameters.

An increase of $\Lambda$ favors the lack of luminescence.[48,49] The critical value $\Lambda_c$ where luminescence disappears depends, however, on the electronic structure of the excited state. In the case of $Mn^{2+}$-doped fluorite lattices[50,51] where the first excited state has a long lifetime the critical value is $\Lambda_c = 0.07$, while for $F$ centers[52] $\Lambda_c = 0.25$. In the case of $Mn^{2+}$-doped fluoroperovskites when $R_e$ increases both $E_s$ and $E_G$ increase, leading to a small increase of $\Lambda$ along the series. More precisely,[19,50] $\Lambda = 0.033$ for $KMgF_3:Mn^{2+}$, while $\Lambda = 0.039$ for $RbCdF_3:Mn^{2+}$. Therefore, in these systems, an increase of the chemical pressure leads to a slight decrement of $\Lambda$ favoring the existence of luminescence through the whole series as the $\Lambda$ variation is *only* of 15%.

According to the present results, the effects of a hydrostatic pressure upon $\Lambda$ would also be different to those coming from chemical pressures. For instance, considering the results on $E_s$ gathered in Fig. 3, an *increase* of $\Lambda$ up to $\Lambda \approx 0.05$ can be expected for $KMgF_3:Mn^{2+}$ when the applied pressure makes $\Delta R_e/R_e = -10\%$. Although this figure is higher than $\Lambda = 0.033$ measured at ambient pressure, it is, however, smaller than $\Lambda_e = 0.07$ as derived[50] from the results on $Mn^{2+}$-doped $SrF_2$ and $BaF_2$, and thus luminescence would be in principle not fully quenched. Further experimental work about this matter is desirable.

## IV. FINAL REMARKS

Variations of the $A_{1g}$ and $E_g$ frequencies of $MnF_6{}^{4-}$ along the series of cubic $ABF_3$ perovskites are calculated to be much bigger than those coming from a hydrostatic pressure applied on a given system like $KMgF_3:Mn^{2+}$ and those corresponding to the $LO_3$ frequency of the host lattice.[27] These results allow one to understand the experimental increase of the Stokes shift associated with the $MnF_6{}^{4-}$ unit when the host lattice parameter $a$ increases[19] and also the nature of vibrations observed[24] in the high-resolution optical spectra on $KBF_3:Mn^{2+}$ $(B\text{:Mg, Zn})$. According to the present findings, such vibrational modes have a dominant local character similar to that found for $Cr^{3+}$ in elpasolites.[13–15] It was early pointed out by Sturge[53] that vibrational modes involved in progressions seen in optical spectra of transition-metal impurities exhibit a local or quasilocal character. The conclusions reached in this work thus support that view. The distinct role played by local and host lattice modes is also well seen in experiments[54] on the nonradiative decay in $Mg_2SiO_4:Cr^{4+}$. In a first step such a decay is found to involve the excitation of local modes. This energy is *later* transferred to the vibrational modes of host lattice.

Despite the present study accounting for the main trends displayed by optical spectra of $ABF_3:Mn^{2+}$ systems, the influence of cluster size and the addition of further shells[55–57] to the description of $A_{1g}$ and $E_g$ modes deserve a supplementary investigation.

The present findings can also be useful for understanding the Stokes shift (and its dependence on hydrostatic or chemical pressures) of other $3d$ impurities in high-symmetry lattices where the impurity is sixfold coordinated.[58,59] Recent experimental data on $Cr^{3+}$ in several cubic chloroelpasolites[60] reveal that the Jahn-Teller energy $E_{JT}$ in the ${}^4T_2$ first excited state decreases when $R_e$ does. As $E_{JT}$ is just equal[45,12,13,15] to $S_E\hbar\omega_E$, such a variation is thus qualitatively similar to that derived for *cubic* fluoroperovskites doped with Mn$^{2+}$.

The relevance of knowing the $R_e$ dependence of parameters like $E_s$ or $S_i$ $(i=A,E)$ in order to explain the pressure-induced variations of optical properties has recently been pointed out.[61] According to the analysis carried out in Sec. III C, one would expect[14,15] that $S_A$ and $S_E$ would decrease when a hydrostatic pressure is applied provided pressure does not favor a distortion of the initial geometry. In $Cs_2NaScCl_6$:Cr$^{3+}$ where $CrCl_6{}^{3-}$ remains cubic under pressure, $S_A$ and $S_E$ are recently found[62] to experience a decrement when pressure increases. By contrast, in $Mg_2SiO_4$:Cr$^{4+}$ the average Huang-Rhys factor of the emission band is found to increase[63] when pressure goes from to 9 to 12 GPa. This increase has been ascribed[63] to the appearance of bigger distortions on the $CrO_4{}^{4-}$ unit induced by the hydrostatic pressure.

Usually, when two *pure* compounds contain isoelectronic complexes with the same ligand, vibrational frequencies increase with the metal oxidation state.[64] Nevertheless, the $\omega_A$ frequency derived for $KMgF_3$:Mn$^{2+}$ is quite comparable to that for compounds[62,47] involving $FeF_6{}^{3-}$ units. It is worth noting, however, that when $R_e$ is closer to the sum of ionic radii of F$^-$ and Mn$^{2+}$ (212 pm), then $\hbar\omega_A$ is certainly smaller and close to $\sim$400 cm$^{-1}$ as estimated[12] for $RbMnF_3$. This comparison stresses once more the relevant effects that chemical pressures can produce upon the properties of an impurity. The comparison between the experimental[28] and calculated $\gamma_A$ for $CrF_6{}^{3-}$ in elpasolites supports the use of simple clusters for deriving reasonable values of Grüneisen constants in the case of impurities in insulating lattices. When the Grüneisen constant of the $A_1$ mode is computed from the potential energy curve calculated with all ions fixed except the ligands, then the obtained value could, however, be significantly smaller than the right one. It is worth noting that using Eqs. (16) and (17) a ratio $\gamma_A(f)/\gamma_A$ close to 0.5 is obtained even if $g' \ll g$ provided $g'/g \approx k'/k$ holds. This idea can thus explain in a simple way the results discussed in Sec. III B and also the value of $\gamma_A = 0.91$ reported in Ref. 35 for $CrF_6{}^{3-}$ in $K_2NaGaF_6$:Cr$^{3+}$, which can be compared to the experimental value[28] $\gamma_A = 1.9$.

From the present results it can be expected that in systems containing impurities like Cu$^{2+}$, Ag$^{2+}$, or Rh$^{2+}$ where the Jahn-Teller coupling can occur in the *ground state*[65] chemical and hydrostatic pressures can also lead to different situations. Work along this line is now under way.

## ACKNOWLEDGMENTS

Fruitful discussions with Dr. F. Rodríguez are acknowledged. The authors are indebted to Dr. R. Valiente for information about optical experiments on $Cs_2NaScCl_6$:Cr$^{3+}$ under hydrostatic pressure. This work has been supported by the CICYT under Project No. PB98-0190.

---

[1] S. Sugano and R. G. Shulman, Phys. Rev. **130**, 517 (1963).

[2] S. Sugano, Y. Tanabe, and H. Kamimura, *Multiplets of Transition-Metal Ions in Crystals* (Academic, New York, 1970).

[3] K. Pierloot, E. Van Praet, and L. G. Vanquickenborne, J. Chem. Phys. **96**, 4163 (1992).

[4] J. A. Aramburu and M. Moreno, Phys. Rev. B **56**, 604 (1997).

[5] H. Drickamer, J. Chem. Phys. **47**, 1880 (1967).

[6] F. Rodriguez and M. Moreno, J. Chem. Phys. **84**, 692 (1986).

[7] S. J. Duclos, Y. K. Vohra, and A. L. Ruoff, Phys. Rev. B **41**, 5372 (1990).

[8] B. Villacampa, R. Cases, V. M. Orera, and R. Alcalá, J. Phys. Chem. Solids **55**, 263 (1994).

[9] M. C. Marco de Lucas, F. Rodríguez, C. Prieto, M. Verdaguer, and H. U. Güdel, J. Phys. Chem. Solids **56**, 995 (1995).

[10] D. Hernández, F. Rodríguez, M. Moreno, and H. U. Güdel, Physica B **265**, 186 (1999).

[11] Y. Mita, Y. Sakai, D. Izaki, M. Kobayashi, S. Endo, and S. Mochizuki, Phys. Status Solidi B **223**, 247 (2001).

[12] E. I. Solomon and D. S. McClure, Phys. Rev. B **9**, 4690 (1974).

[13] R. Knochenmuss, C. Reber, M. V. Rajasekharan, and H. U. Güdel, J. Chem. Phys. **85**, 4280 (1986).

[14] M. Moreno, J. A. Aramburu, and M. T. Barriuso, J. Phys.: Condens. Matter **4**, 9481 (1992).

[15] M. T. Barriuso, J. A. Aramburu, and M. Moreno, Phys. Status Solidi B **193**, 193 (1996).

[16] M. A. Buñuel, R. Alcala, and R. Cases, J. Chem. Phys. **109**, 2294 (1998).

[17] M. Marsman, J. Andriessen, and C. W. E. van Eijk, Phys. Rev. B **61**, 1 (2000).

[18] J. J. Rousseau, A. Leble, and J. C. Fayet, J. Phys. (Paris) **39**, 1215 (1978).

[19] M. Marco de Lucas, F. Rodríguez, and M. Moreno, Phys. Rev. B **50**, 2760 (1994).

[20] F. Lahoz, P. J. Alonso, R. Alcala, T. Pawlik, and J. M. Spaeth, J. Phys.: Condens. Matter **7**, 8637 (1995).

[21] A. Leblé, Ph.D. thesis, Université du Maine, 1982.

[22] M. T. Barriuso and M. Moreno, Phys. Rev. B **29**, 3623 (1984).

[23] M. T. Barriuso, J. A. Aramburu, and M. Moreno, J. Phys.: Condens. Matter **11**, L525 (1999).

[24] F. Rodríguez, H. Riesen, and H. U. Güdel, J. Lumin. **50**, 101 (1991).

[25] M. Marco de Lucas, F. Rodríguez, and M. Moreno, J. Phys.: Condens. Matter **7**, 7535 (1995).

[26] C. Ridou, M. Rousseau, J. Bouillot, and C. Vettier, J. Phys. C **17**, 1001 (1984).

[27] S. Salaun and M. Rousseau, Phys. Rev. B **51**, 15 867 (1995).

[28] J. F. Dolan, A. G. Rinzler, L. A. Kappers, and R. H. Bartram, J. Phys. Chem. Solids **53**, 905 (1992).

[29] G. te Velde and E. J. Baerends, J. Comput. Phys. **99**, 84 (1992).

[30] A. D. Becke, Phys. Rev. A **38**, 3098 (1988).

[31] J. P. Perdew, Phys. Rev. B **33**, 8822 (1986).

[32] I. Bersuker and V. Z. Polinger, in *The Dynamical Jahn-Teller Effect in Localized Systems*, edited by Yu Perlin and W. Wagner (North-Holland, Amsterdam, 1984).

[33] R. G. Parr and W. Yang, *Density-Functional Theory of Atoms and*

*Molecules* (Oxford University Press, New York, 1989), p. 141.
[34] F. M. Michel-Calendini, K. Bellafrouh, and H. Chermette, Phys. Rev. B **50**, 12 326 (1994).
[35] F. Deghoul, H. Chermette, F. Rogemond, R. Moncorge, C. Stuckl, and C. Daul, Phys. Rev. B **60**, 2404 (1999).
[36] J. A. Aramburu, M. Moreno, K. Doclo, C. Daul, and M. T. Barriuso, J. Chem. Phys. **110**, 1497 (1999).
[37] L. Seijo, Z. Barandiarán, and L. G. M. Petterson, J. Chem. Phys. **98**, 4041 (1993).
[38] P. Brüesch, *Phonons: Theory and Experiments I* (Springer, Berlin, 1982).
[39] C. J. Ballhausen, *Introduction to Ligand Field Theory* (McGraw-Hill, New York, 1962).
[40] P. Bouvier and G. Lucazeau, J. Phys. Chem. Solids **61**, 569 (2000).
[41] S. Biernacki and M. Scheffler, Phys. Rev. Lett. **63**, 290 (1989).
[42] C. Hu, C. Wang, C. Chan, and K. Ho, Phys. Rev. B **43**, 5024 (1991).
[43] D. Groh, R. Pandey, and J. Recio, Phys. Rev. B **50**, 14 860 (1994).
[44] V. Goldberg, R. Moncorge, D. Pacheco, and B. Di Bartolo, *Luminiscence of Inorganic Solids* (Plenum, New York, 1978).
[45] F. S. Ham, Phys. Rev. **138**, B1727 (1965).
[46] M. Moreno, J. A. Aramburu, and M. T. Barriuso, Phys. Rev. B **56**, 14 423 (1997).
[47] J. A. Aramburu, J. I. Paredes, M. T. Barriuso, and M. Moreno, Phys. Rev. B **61**, 6525 (2000).
[48] D. L. Dexter, C. C. Klick, and G. A. Russell, Phys. Rev. **100**, 603 (1955).
[49] C. Reber and H. U. Güdel, J. Lumin. **47**, 7 (1990).
[50] M. C. Marco de Lucas, M. Moreno, F. Rodríguez, and P. G. Baranov, J. Phys.: Condens. Matter **8**, 2457 (1996).
[51] M. Diaz, F. Lahoz, B. Villacampa, R. Cases, B. Sobolev, and R. Alcalá, J. Lumin. **81**, 53 (1999).
[52] R. H. Bartram and M. Stoneham, Solid State Commun. **17**, 1593 (1975).
[53] M. D. Sturge, Solid State Phys. **20**, 91 (1967); Solid State Commun. **9**, 899 (1971).
[54] D. M. Calistru, S. G. Demos, and R. R. Alfano, Phys. Rev. Lett. **78**, 374 (1997).
[55] A. Barker and A. J. Sievers, Rev. Mod. Phys. **47**, Suppl. No. 2, FS1 (1975).
[56] V. Luaña, M. Florez, and L. Pueyo, J. Chem. Phys. **99**, 7970 (1993).
[57] V. I. Sokolov, E. A. Shirokov, A. N. Kislov, and V. G. Mazurenko, Phys. Status Solidi B **221**, 553 (2000).
[58] G. Blasse and B. C. Grabmaier, *Luminescent Materials* (Springer-Verlag, Berlin, 1994).
[59] Dong-Ping Ma and D. E. Ellis, J. Lumin. **71**, 329 (1997).
[60] O. S. Wenger and H. U. Güdel, J. Chem. Phys. **114**, 5832 (2001).
[61] K. L. Bray, Top. Curr. Chem. **213**, 1 (2001).
[62] O. S. Wenger, R. Valiente, and H. U. Güdel, J. Chem. Phys. **115,** 3819 (2001).
[63] Y. Shen and K. L. Bray, Phys. Rev. Lett. **84**, 3990 (2000).
[64] K. Nakamoto, *Infrared and Raman Spectra of Inorganic and Coordination Compounds*, 4th ed. (Wiley, New York, 1986).
[65] W. Grochala and R. Hoffmann, Angew. Chem. Int. Ed. Engl. **40**, 4000 (2001).